

## Stabilization of $\beta$ -Catenin Induces Pancreas Tumor Formation

PATRICK W. HEISER,\* DAVID A. CANO,\* LIMOR LANDSMAN,\* GRACE E. KIM,<sup>†</sup> JAMES G. KENCH,<sup>§,||</sup> DAVID S. KLIMSTRA,<sup>||</sup> MAKETO M. TAKETO,<sup>#</sup> ANDREW V. BIANKIN,<sup>\*\*</sup> and MATTHIAS HEBROK\*

\*Diabetes Center, University of California, San Francisco; <sup>†</sup>Department of Pathology, University of California, San Francisco; <sup>§</sup>Cancer Research Program, Garvan Institute of Medical Research, Sydney, New South Wales, Australia; <sup>||</sup>Department of Tissue Pathology, Institute of Clinical Pathology and Medical Research, Westmead Hospital, Westmead, New South Wales, Australia; <sup>††</sup>Department of Pathology, Memorial Sloan Kettering Cancer Center, New York, New York; <sup>#</sup>Department of Pharmacology, Graduate School of Medicine, Kyoto University, Kyoto, Japan; <sup>\*\*</sup>Department of Surgery, Bankstown Hospital, Sydney, New South Wales, Australia

**Background & Aims:**  $\beta$ -Catenin signaling within the canonical Wnt pathway is essential for pancreas development. However, the pathway is normally down-regulated in the adult organ. Increased cytoplasmic and nuclear localization of  $\beta$ -catenin can be detected in nearly all human solid pseudopapillary neoplasms (SPN), a rare tumor with low malignant potential. Conversely, pancreatic ductal adenocarcinoma (PDA) accounts for the majority of pancreatic tumors and is among the leading causes of cancer death. Whereas activating mutations within  $\beta$ -catenin and other members of the canonical Wnt pathway are rare, recent reports have implicated Wnt signaling in the development and progression of human PDA. Here, we sought to address the role of  $\beta$ -catenin signaling in pancreas tumorigenesis. **Methods:** Using Cre/lox technology, we conditionally activated  $\beta$ -catenin in a subset of murine pancreatic cells in vivo. **Results:** Activation of  $\beta$ -catenin results in the formation of large pancreatic tumors at a high frequency in adult mice. These tumors resemble human SPN based on morphologic and immunohistochemical comparisons. Interestingly, stabilization of  $\beta$ -catenin blocks the formation of pancreatic intraepithelial neoplasia (PanIN) in the presence of an activating mutation in Kras that is known to predispose individuals to PDA. Instead, mice in which  $\beta$ -catenin and Kras are concurrently activated develop distinct ductal neoplasms that do not resemble PanIN lesions. **Conclusions:** These results demonstrate that activation of  $\beta$ -catenin is sufficient to induce pancreas tumorigenesis. Moreover, they indicate that the sequence in which oncogenic mutations are acquired has profound consequences on the phenotype of the resulting tumor.

ber of human cancers.<sup>1–3</sup> In the absence of Wnt ligand,  $\beta$ -catenin is targeted for degradation by phosphorylation via its interaction with a complex containing Axin and APC. However, upon binding of Wnt ligand, this complex is inhibited, unphosphorylated  $\beta$ -catenin accumulates in the cytoplasm, and this protein isoform eventually enters the nucleus. After nuclear entry, this stabilized, or “activated,” form of  $\beta$ -catenin binds Tcf/Lef transcriptional coactivators resulting in up-regulation of Wnt-responsive target genes (reviewed in Reya and Clevers<sup>4</sup> and Widelitz<sup>5</sup>).

Several recent studies have demonstrated that the canonical Wnt signaling pathway is dynamically regulated during pancreatic development, and that  $\beta$ -catenin, in particular, is essential for normal pancreatic organogenesis.<sup>6–10</sup> However, this pathway is normally down-regulated within the adult pancreas.<sup>6,7</sup>

Mutations in  $\beta$ -catenin/APC and/or evidence of aberrant canonical Wnt signaling pathway activity have been found in pancreatoblastomas,<sup>11</sup> acinar cell carcinoma,<sup>12</sup> pancreatic ductal adenocarcinoma (PDA),<sup>13–15</sup> and solid pseudopapillary neoplasm (SPN).<sup>16–19</sup> However, a direct causal relationship between Wnt pathway deregulation and tumor development has not been clearly demonstrated in any of these tumor types.

Herein, we demonstrated that stabilization of  $\beta$ -catenin within the pancreatic epithelium, including duct cells, results in the formation of tumors that resemble human SPN. Surprisingly, concurrent activation of  $\beta$ -catenin and Kras, a mediator of PDA formation, prevents the formation of pancreatic intraepithelial neoplasia (PanINs) and PDA. Thus, our data present in vivo evidence that increased Wnt signaling is sufficient to induce pancreatic tumor formation and that the se-

$\beta$ -Catenin plays 2 divergent, yet critical, cellular roles. The first is at the plasma membrane, where it interacts with cadherins to form adherens junctions that are important for cell–cell adhesion. The second is at the center of the canonical Wnt signaling pathway, a signaling cascade that is essential for embryonic development and whose dysregulation has been implicated in a num-

**Abbreviations used in this paper:** ITT, intraductal tubular tumor; MAPK, mitogen-activated protein kinase; PDA, pancreatic ductal adenocarcinoma; SPN, solid pseudopapillary neoplasms; PanIN, pancreatic intraepithelial neoplasia.

© 2008 by the AGA Institute

0016-5085/08/\$34.00

doi:10.1053/j.gastro.2008.06.089

quence of oncogene activation is critically important for the formation of different types of tumors.

## Materials and Methods

### Mice

Noon of the day when vaginal plugs are detected is treated as e0.5 day post coitum. The following mouse lines were used:  $\beta$ -cat<sup>active</sup>, carrying the floxed exon 3 allele of  $\beta$ -catenin,<sup>20</sup> Kras<sup>G12D</sup> mice, carrying a targeted mutation in the first exon of the Kras allele,<sup>21</sup> and the R26R<sup>22</sup> and Z/AP<sup>23</sup> reporter lines. All lines require Cre-mediated recombination for transgene expression and were crossed with strains expressing Cre-recombinase under the control of the endogenous *Ptf1a* promoter<sup>24</sup> or the Pdx1 promoter (*Pdx-Cre<sup>early</sup>*)<sup>25</sup> and maintained in a mixed background. All transgenic mice used carry a single copy of the indicated transgene.

### Tissue Preparation, Immunohistochemistry, and Microscopy

Embryonic tissues were fixed and paraffin wax imbedded as previously described.<sup>26</sup> Adult murine pancreas and tumor tissue was fixed overnight at 4°C in 1× zinc-buffered formalin (Anatech, Ltd., Battle Creek, MI). Hematoxylin and eosin staining and immunohistochemical and immunofluorescence analyses were performed as previously described<sup>27</sup> on 6- $\mu$ m sections.

Staining for  $\beta$ -galactosidase activity in whole e11.5 embryos was performed as previously described.<sup>28</sup> Alkaline phosphatase and Alcian blue staining methods, antibodies used, morphometric quantitation protocols, quantitative polymerase chain reaction (PCR) conditions, primer sequences, and Western blotting conditions are provided in the Supplemental Methods section (see Supplementary material online at [www.gastrojournal.org](http://www.gastrojournal.org)).

## Results

### Ptf1a-Cre Mice Target a Subset of Early Pancreatic Progenitor Cells and Pancreatic Ducts

Previously, we demonstrated that stabilization of  $\beta$ -catenin within most cells of the early pancreatic epithelium using the *Pdx-Cre<sup>early</sup>* mouse severely disrupts pancreas development leading to neonatal lethality. In contrast, delayed expression of  $\beta$ -cat<sup>active</sup> under the control of a different *Pdx1* promoter (*Pdx-Cre<sup>late</sup>*) mainly targets acinar, but not ductal, cells. In this context, activation of  $\beta$ -catenin results in a significant increase in acinar cell number without evidence of cellular transformation.<sup>28</sup> To test whether the *Ptf1a* promoter, another pancreatic transcription factor, would allow stabilization of  $\beta$ -catenin within a subset of early pancreatic epithelial cells that include duct progenitors, we directly compared the pattern of Cre-recombinase activity in *Pdx-Cre<sup>early</sup>* and *Ptf1a-Cre* mice. For this purpose, we used 2 reporter strains,

R26R<sup>22</sup> and Z/AP<sup>23</sup> that express  $\beta$ -galactosidase or alkaline phosphatase, respectively, on Cre-mediated recombination.

We found that, like the *Pdx-Cre<sup>early</sup>* mouse strain (Figure 1A), the *Ptf1a-Cre* strain has detectable Cre recombinase activity resulting in  $\beta$ -galactosidase staining at e11.5 (Figure 1C), a time point when ductal progenitors are still being specified.<sup>25</sup> However, although the *Pdx-Cre<sup>early</sup>* mouse has robust Cre-recombinase activity in the majority of cells within the pancreatic epithelium (Figure 1B), only a subset of epithelial cells are targeted by the *Ptf1a-Cre* strain (Figure 1D, black arrows) at this time point. These results are consistent with previous reports.<sup>24</sup>

By 4 weeks of age, the majority of acinar cells within both the *Pdx-Cre<sup>early</sup>* and *Ptf1a-Cre*; Z/AP mice are positive for alkaline phosphatase (Figure 1E). In addition, pancreatic ducts contain cells that have alkaline phosphatase activity in those mice (Figure 1E, yellow arrows). A subset of pancreatic ducts in the *Ptf1a-Cre*; Z/AP mouse do not show evidence of Cre-recombinase activity and are not positive for alkaline phosphatase (Figure 1E, red arrow). Sections from control animals did not exhibit detectable alkaline phosphatase activity within the acinar or ductal compartments (Figure 1E). Thus, the limited Cre-expression domain within the early pancreas, when  $\beta$ -catenin stabilization is likely to disrupt organogenesis, coupled with effective targeting of pancreatic ductal cells, make this mouse line well-suited to probe the effects of  $\beta$ -catenin stabilization in adult mice.

### Activation of $\beta$ -Catenin in Ptf1a-Cre; $\beta$ -cat<sup>active</sup> Mice Causes Ductal Lesions and Increased Pancreas Mass

Consistent with our reporter mouse analysis, only a subset of cells within the early pancreatic epithelium of the *Ptf1a-Cre*;  $\beta$ -cat<sup>active</sup> mice exhibit evidence of  $\beta$ -catenin activation (Supplemental Figure 1C; see Supplementary material online at [www.gastrojournal.org](http://www.gastrojournal.org)). At birth, the gross pancreatic morphology of *Ptf1a-Cre*;  $\beta$ -cat<sup>active</sup> seems similar to control (data not shown). Pancreatic mass is also equivalent at this time point (Figure 2F, graph inset), suggesting that activation of  $\beta$ -catenin within the small number of cells of the early pancreatic epithelium in the *Ptf1a-Cre*;  $\beta$ -cat<sup>active</sup> compared with the widespread activation in the *Pdx-Cre<sup>early</sup>*;  $\beta$ -cat<sup>active</sup><sup>28</sup> is not sufficient to disrupt pancreas formation (Supplemental Figure 1 B and C).

At P0, prominent ductal-associated lesions are visible throughout the pancreas of the *Ptf1a-Cre*;  $\beta$ -cat<sup>active</sup> mice (Figure 2B). These lesions are not seen in control mice (Figure 2A) or in *Pdx-Cre<sup>late</sup>*;  $\beta$ -cat<sup>active</sup>, which do not have any Cre activity in pancreatic ducts.<sup>28</sup> High levels of nuclear-localized  $\beta$ -catenin are seen within these ductal associated lesions (Figure 2D), whereas  $\beta$ -catenin is found exclusively at the plasma membrane in control animals (Figure 2C). Despite their proximity to ductal structures, cells within the lesion that have elevated levels

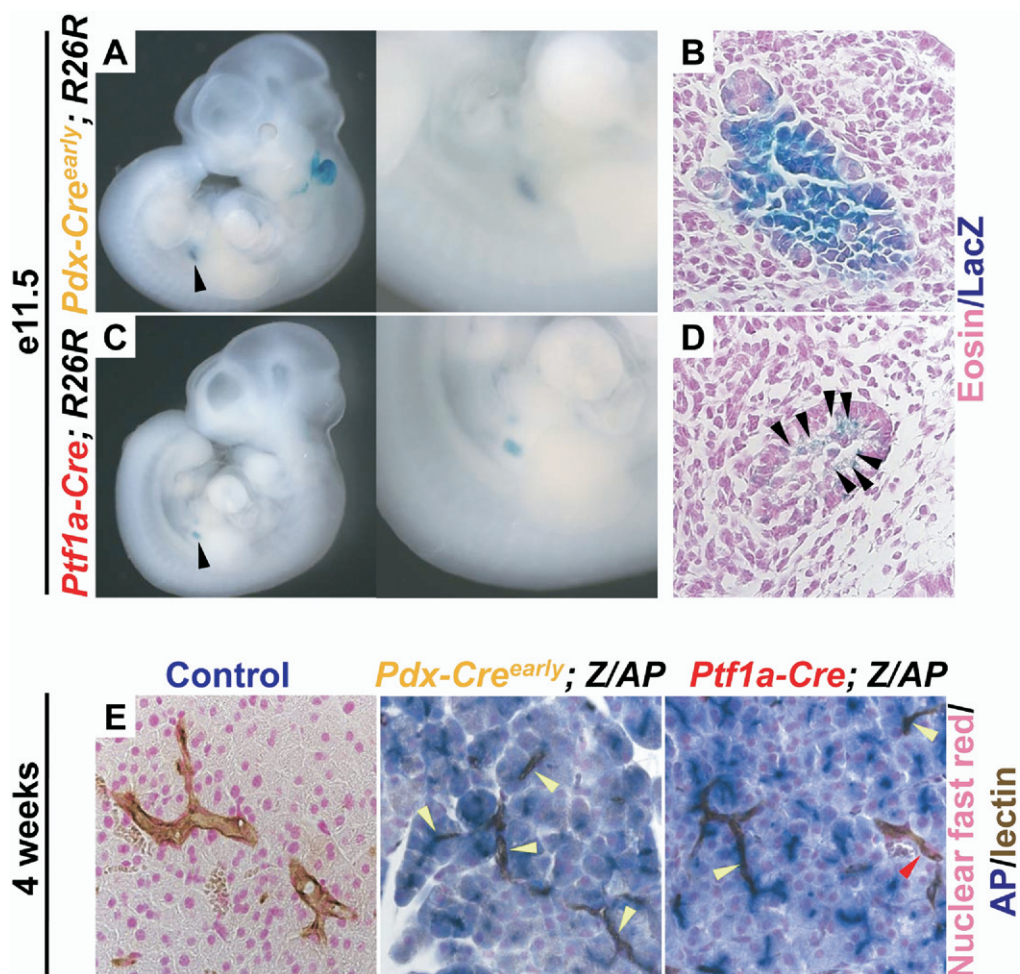


**Figure 1.** *Ptf1a-Cre* mice target a subset of early pancreatic progenitor cells and pancreatic ducts. Staining for *lacZ* marks cells that have undergone Cre mediated recombination in *Pdx-Cre<sup>early</sup>* and *Ptf1a-Cre; R26R* mice. (A–D) e11.5 mouse embryos enzymatically stained for  $\beta$ -galactosidase activity. (A) *Pdx-Cre<sup>early</sup>; R26R*, staining visible in the pancreas, indicated by *black arrow*, and enlarged. (C) *Ptf1a-Cre; R26R*, staining visible in the pancreas, indicated by a *black arrow*, and enlarged. (B, D) Histologic examination of *lacZ* stained sections counterstained with eosin. (B) The majority of cells within the pancreatic epithelium of the *Pdx-Cre<sup>early</sup>; R26R* are positive for  $\beta$ -galactosidase activity. (D) Equivalent sections of a *Ptf1a-Cre; R26R* reveal that only a subset of cells within the pancreatic epithelium are positive for  $\beta$ -galactosidase activity (*black arrows*). Staining for alkaline phosphatase (AP) marks cells that have undergone recombination in 4-week-old *Pdx-Cre<sup>early</sup>; Z/AP* and *Ptf1a-Cre; Z/AP* mice. (E) Histologic sections that have been enzymatically stained for alkaline phosphatase activity (*blue*), DBA lectin to mark pancreatic ducts (*brown*), and nuclear fast red as a counterstain (*pink*). No AP activity is detectable in the control pancreas. The majority of acinar cells and most cells within pancreatic ducts (*yellow arrows*) exhibit clear alkaline phosphatase activity in the *Pdx-Cre<sup>early</sup>; Z/AP* mouse. Almost all acinar cells and a subset of cells within pancreatic ducts (*yellow arrows*) have alkaline phosphatase activity in the *Ptf1a-Cre; Z/AP* mouse. Some pancreatic ducts do not contain cells that are positive for alkaline phosphatase (*red arrow*).

of  $\beta$ -catenin do not express the ductal marker, mucin 1 (Figure 2D). Formal proof of the ductal origin of these cells is not possible without cell lineage tracing experiments. However, the location of these cells suggests a ductal source, indicating that activation of  $\beta$ -catenin may have caused some loss of differentiation in this population.

Although pancreas morphology and mass is normal at P0, 1-month-old *Ptf1a-Cre;  $\beta$ -cat<sup>active</sup>* exhibit a grossly enlarged pancreas that is 4 times greater in mass than control (Figure 2E). Pancreas mass continues to increase with age in the *Ptf1a-Cre;  $\beta$ -cat<sup>active</sup>* (Figure 2F), similar to what we have previously seen in *Pdx-Cre<sup>late</sup>;  $\beta$ -cat<sup>active</sup>* mice.

### ***Ptf1aCre $\beta$ cat<sup>active</sup> Develop Large Pancreatic Tumors at a High Frequency***

Pancreatic tumors are not observed in *Pdx-Cre<sup>late</sup>;  $\beta$ -cat<sup>active</sup>* mice despite the dramatic increase in pancreatic mass.<sup>28</sup> However, large, well-encapsulated tumors are detectable at the gross morphologic level in *Ptf1a-Cre;  $\beta$ -cat<sup>active</sup>* mice by 3 months of age (Figure 3A). These tumors are slow growing and nonmetastatic; moreover, affected animals continue to eat and groom normally. By 12 months, nearly half of all mice exhibit large tumors, which are most often found in the ventral pancreas (Figure 3B).

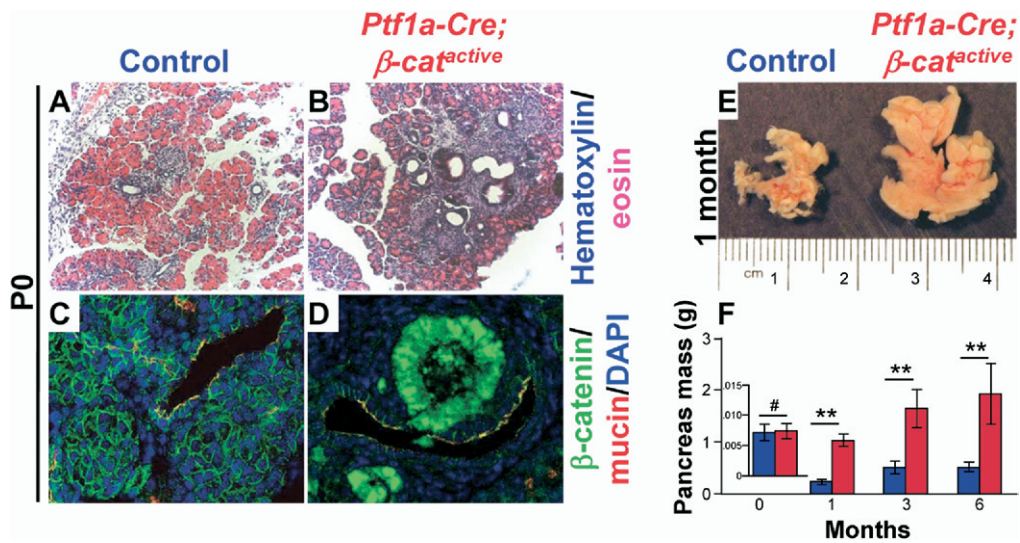


**Figure 2.** Activation of  $\beta$ -catenin in *Ptf1a-Cre; beta-cat<sup>active</sup>* mice causes ductal lesions and increased pancreas mass. Hematoxylin and eosin staining of pancreatic sections from P0 reveals the presence of prominent ductal lesions in the pancreata of *Ptf1a-Cre; beta-cat<sup>active</sup>* mice (B) that are not observed in the pancreata of control littermates (A). Strong nuclear accumulation of  $\beta$ -catenin (green) is seen in these ductal associated (duct labeled by mucin in red) lesions (D), whereas in control animals,  $\beta$ -catenin (green) remains localized to the plasma membrane in pancreatic ducts (C, ducts labeled by mucin in red). Cells that have nuclear localized  $\beta$ -catenin do not co-express mucin. Pancreata from *Ptf1a-Cre; beta-cat<sup>active</sup>* are significantly enlarged when compared with control at 1 month of age (E). Quantitative measurements revealed an approximately 4-fold increase in pancreatic mass at 6 months of age (F;  $n \geq 7$  for each time point analyzed; control, blue; *Ptf1a-Cre; beta-cat<sup>active</sup>*, red). Confidence intervals were calculated using Student's *t*-test. *P* values: #not significant; \*\* $P < .01$ . Error bars represent standard error of the mean.

In cross-section at the gross and histologic levels, areas of necrosis (Figure 3C, yellow), cystic structures (Figure 3C and E\*), and solid, pseudopapillary regions (Figure 3C and E#) are visible. Some pancreas tissue, including acinar and islet structures, remains attached to the outer capsule of the tumor (Figure 3E, arrows).

Although E-cadherin expression and membrane localization in the *Ptf1a-Cre; beta-cat<sup>active</sup>* pancreas is equivalent to control (Supplemental Figure 2A and B and Supplemental Figure 3A; see Supplementary material online at [www.gastrojournal.org](http://www.gastrojournal.org)), its expression is down-regulated within the tumors seen in those mice (Supplemental Figures 2C and 3A). The Wnt target genes Axin2, cyclin D1, and p21 are significantly up-regulated in the pancreata of *Ptf1a-Cre; beta-cat<sup>active</sup>* mice when compared with controls (Figure 3D and F; Supplemental Figure 3D), indicating that stabilization of  $\beta$ -catenin has resulted in robust activation of the canonical Wnt signaling pathway. Tumors isolated from *Ptf1a-Cre; beta-cat<sup>active</sup>* demonstrated an even greater increase in both Axin2 and cyclin D1 expression (Figure 3D and F), as well as significant up-regulation of p21, Cdk4, and c-jun expression (Supplemental Figure 3B–D), suggesting that further deregulation of the canonical Wnt pathway may be occurring during tumorigenesis.

**Tumors in *Ptf1aCre beta-cat<sup>active</sup>* Mice Are Morphologically Similar to Human SPN of the Pancreas**

Based on published reports, up-regulation of  $\beta$ -catenin is often seen in human SPN of the pan-

creas.<sup>16,17</sup> Moreover, activating mutations within the third exon of the human  $\beta$ -catenin gene are also found in the majority of SPNs.<sup>18</sup> Therefore, we directly compared the morphology of a collection of human SPN tissue and the tumors observed in *Ptf1a-Cre; beta-cat<sup>active</sup>* mice.

We found that the mouse tumors recapitulated microscopic features that characterize SPNs in humans. Like the human tumors, all of the mouse tumors were well-circumscribed with a distinct fibrous capsule (Figure 4A and B, black arrows). Moreover, they exhibited extensive necrosis (Figure 4C and D, red arrow) and hemorrhage (Figure 4C and D, black arrows) centrally with preserved tissue typically being found at the periphery (Figure 4A and B). The tumor cells in the subcapsular region were arranged in solid sheets and the intervening spaces were filled with hemorrhage or necrotic debris. No glandular spaces were present. Focal calcifications were observed in 1 mouse tumor (data not shown), a feature that is sometimes seen in human SPN (Figure 4C, green arrow). As in human SPNs (Figure 4E and F) the mouse tumor cells were small, polygonal, and monomorphic with a moderate amount of clear or pale eosinophilic cytoplasm. In addition, the mouse tumor cell nuclei were round to ovoid with dispersed, finely granular chromatin and inconspicuous nucleoli, features that are very similar to those seen in human SPN (Figure 4E and F). Mitotic figures were rare in both human and mouse tumors.

In contrast to human cases of SPN, no eosinophilic hyaline globules or cholesterol clefts were identified in the mouse tumors, although foamy macrophages were

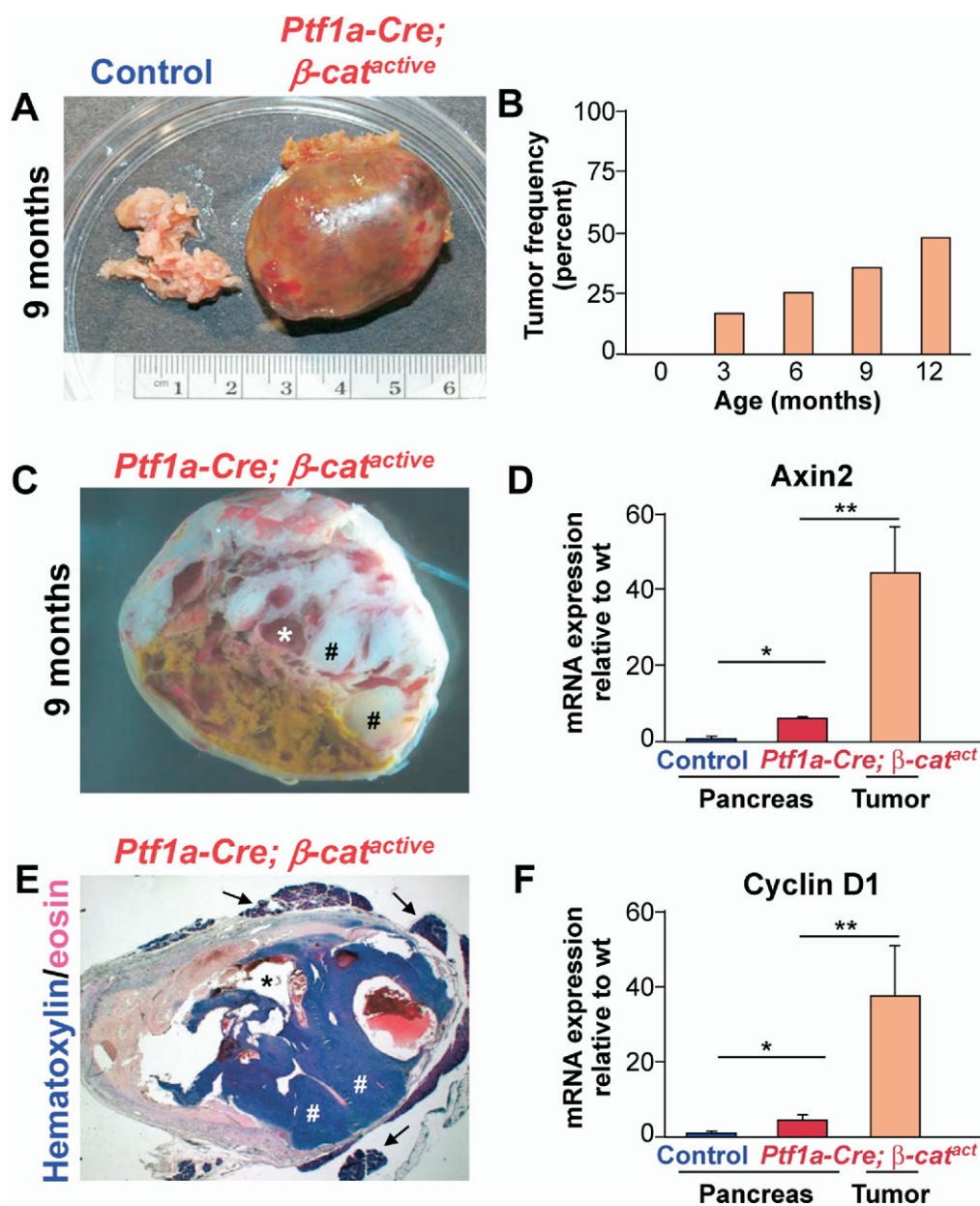


**Figure 3.** *Ptf1a-Cre; β-cat<sup>active</sup>* mice develop large pancreatic tumors at a high frequency. Gross morphology of a typical tumor seen in the pancreas of *Ptf1a-Cre; β-cat<sup>active</sup>*, aged 9 months (A, right) compared with a pancreas from a littermate control (A, left). Gross morphology of a cross-section of the murine tumor reveals pseudopapillary regions (C, labeled by #) and cystic structures (C, labeled by \*). Histologic examination of the murine tumor (original magnification, ×12) shows the pseudopapillary regions (E, labeled by #), cystic structures (E, labeled by \*), and the pancreatic remnant surrounding the tumor (E, labeled by arrow). Tumors are first detectable in *Ptf1a-Cre; β-cat<sup>active</sup>* mice at 3 months of age. By 12 months of age, nearly 50% of *Ptf1a-Cre; β-cat<sup>active</sup>* mice exhibit tumors (B;  $n \geq 8$  for each time point examined). Expression of the Wnt target genes, Axin 2 (D) and cyclin D1 (F) are significantly up-regulated in the *Ptf1a-Cre; β-cat<sup>active</sup>* pancreas when compared with control pancreas at 9 months of age by reverse transcriptase PCR. Tumors found in *Ptf1a-Cre; β-cat<sup>active</sup>* mice exhibit a further increase in overexpression of Axin 2 (D) and cyclin D1 (F). Confidence intervals were calculated using Student's *t*-test ( $n \geq 3$ ). *P* values: #not significant; \**P* < .05; \*\**P* < .01. Error bars represent standard deviation.

often present. Nuclear grooves that are seen in human SPNs were also absent in the mouse tumors. A summary of our comparison of tumor morphology is presented in Supplemental Table 1 (see Supplementary material online at [www.gastrojournal.org](http://www.gastrojournal.org)).

#### **Tumors in *Ptf1a-Cre; β-cat<sup>active</sup>* Mice Have Marker Expression That Is Similar to Human SPN**

To characterize the molecular similarities between our cohort of human SPN tissue and the tumors present within the *Ptf1a-Cre; β-cat<sup>active</sup>* mice, we analyzed the expression of a variety of well-established markers of SPN by immunohistochemistry. The human SPN samples in our collection demonstrated marker expression that is consistent with the published literature. The majority of human

SPNs in our panel (11/13) had clear and dramatic up-regulation of β-catenin, including strong cytoplasmic and nuclear localization (Figure 5A). In comparison, β-catenin is exclusively localized to the plasma membrane in normal human pancreatic tissue (Figure 5A). As expected, all tumors present in the *Ptf1a-Cre; β-cat<sup>active</sup>* have similarly high levels of cytoplasmic and nuclear β-catenin (Figure 5A). In support of the increased expression levels of Wnt target genes (Figure 3; Supplemental Figure 3), β-catenin is more robustly expressed in tumor tissue, than in the pancreas from *Ptf1a-Cre; β-cat<sup>active</sup>* mice, where it remains preferentially partitioned to the nucleus (Figure 5A).

All 13 human SPN samples expressed α-1 anti-trypsin and cyclin D1, whereas normal human pancreatic tissue is largely negative for both markers (Figure 5B and C,

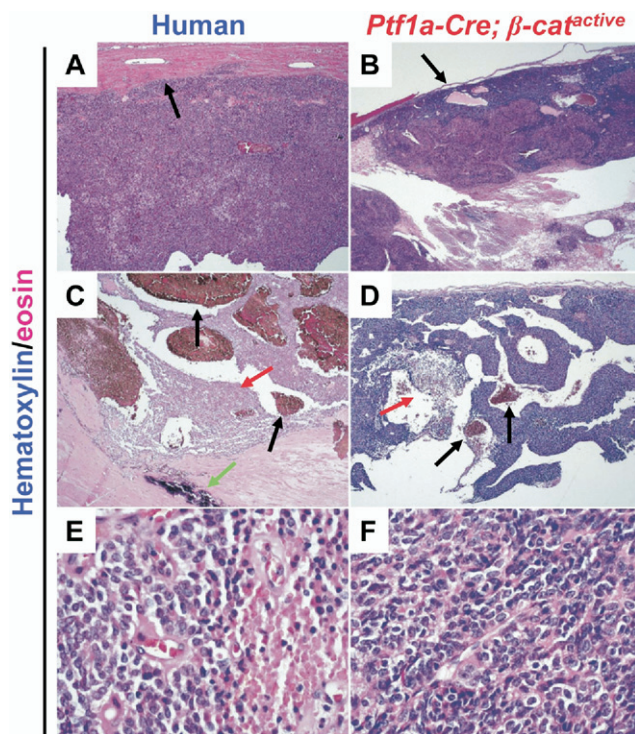


**Figure 4.** Tumors in *Ptfla-Cre;  $\beta$ -cat<sup>active</sup>* mice are morphologically similar to human solid pseudopapillary tumors of the pancreas. Slides were stained with hematoxylin and eosin to provide contrast. Low-power view (original magnification,  $\times 50$ ) of human SPN (A) and murine tumor (B). Black arrows indicate tumor capsule (A,B). Low power view ( $\times 50$ ) of human SPN (C) and murine tumor (D), with black arrows indicating areas of hemorrhage (C, D), red arrows indicating areas of necrosis (C, D), and green arrow to indicate a site of calcification (C). High-power view (original magnification,  $\times 400$ ) of human SPN (E) and murine tumors (F). Images shown are representative samples from 13 human and 6 murine tumors analyzed; mice were 9 months old.

respectively). All tumors analyzed from *Ptfla-Cre;  $\beta$ -cat<sup>active</sup>* mice (6/6) also showed staining for  $\alpha$ -1 anti-trypsin and cyclin D1 that was similar to the human SPN samples (Figure 5B and C, respectively). Whereas the pancreas of *Ptfla-Cre;  $\beta$ -cat<sup>active</sup>* was negative for  $\alpha$ -1 anti-trypsin (Figure 5B) as in the human samples, cyclin D1 staining could be detected within exocrine cells (Figure 5C). This increase is predicted by the quantitative PCR analysis shown previously (Figure 3F). Because cyclin D1 is a critical regulator of cell-cycle progression, its up-regulation in *Ptfla-Cre;  $\beta$ -cat<sup>active</sup>* may be partially responsible for the increase in pancreas mass observed (Figure 2E).

All human and murine tumors tested were also positive for neuron-specific enolase (data not shown), but negative for chromogranin, AE1/AE3, clusterin, or estrogen receptor  $\alpha$  (data not shown). Neither the majority of human tumors (12/13) nor the murine tumors (6/6) expressed synaptophysin, a marker of endocrine differentiation (Figure 5D). Murine tumors also did not express chymotrypsin, a marker of pancreatic exocrine cells (data not shown). The results of this marker comparison are summarized in Supplemental Table 2 (see Supplemen-

tary material online at [www.gastrojournal.org](http://www.gastrojournal.org)). These data demonstrate that the tumors found in *Ptfla-Cre;  $\beta$ -cat<sup>active</sup>* mice closely resemble human SPN at the immunohistochemical level.

### **PanIN Formation Is Blocked in *Ptfla-Cre $\beta$ -cat<sup>active</sup> Kras<sup>G12D</sup>* Mice**

Activating mutations in the GTP-ase *Kras* are found in  $>90\%$  of invasive PDA<sup>29</sup> and are thought to play a critical role in the formation of these highly lethal tumors.<sup>21,30,31</sup> A single amino acid change from glycine to aspartic acid, the most common site of mutation in human PDA, causes constitutive activation of Ras effector pathways. Previous reports using a mouse model, in which expression of the *Kras<sup>G12D</sup>* oncogenic form is mediated by *Ptfla-Cre*, have demonstrated that this mutation alone is sufficient to induce PanIN, the most common precursor lesion to PDA.<sup>21,32,33</sup> Therefore, we asked whether aberrant activation of *Kras* in *Ptfla-Cre;  $\beta$ -cat<sup>active</sup>* mice might convert the SPN-like lesions into a more malignant tumor.

At 3 months of age, *Ptfla-Cre;  $\beta$ -cat<sup>active</sup>, Kras<sup>G12D</sup>* mice have pancreata that are reduced in size compared with controls and *Ptfla-Cre; Kras<sup>G12D</sup>* littermates (Figure 6A). This loss of pancreatic mass in the *Ptfla-Cre;  $\beta$ -cat<sup>active</sup>, Kras<sup>G12D</sup>* is striking given that *Ptfla-Cre;  $\beta$ -cat<sup>active</sup>* mouse littermates exhibit pancreatic hyperplasia (Figure 6A) similar to what was previously described (Figure 2E).

Histologic analysis of the pancreas sections from *Ptfla-Cre;  $\beta$ -cat<sup>active</sup>, Kras<sup>G12D</sup>* mice by hematoxylin and eosin staining reveals a dramatic loss of acinar cells replaced by small dilated ducts, suggestive of acinar to ductal metaplasia (Figure 6B; Supplemental Figure 4D; see Supplementary material online at [www.gastrojournal.org](http://www.gastrojournal.org)). Moreover, the *Ptfla-Cre;  $\beta$ -cat<sup>active</sup>, Kras<sup>G12D</sup>* mouse pancreas exhibits a substantial desmoplastic reaction that is more extensive than what is observed in the *Ptfla-Cre; Kras<sup>G12D</sup>* (confirmed by Gomori trichrome staining; data not shown). These mice also exhibit tumors with 2 distinct morphologic patterns: cribriform and ductal (Figure 6B, yellow \* region with cribriform morphology; yellow # region with ductal morphology; higher magnification pictures are shown in Supplemental Figures 4D, E and F, respectively). Lesions with similar morphology are not seen in the pancreas or in the SPN-like tumors of *Ptfla-Cre;  $\beta$ -cat<sup>active</sup>* mice (Figure 6B; Figure 4F; Supplemental Figure 4B), *Ptfla-Cre; Kras<sup>G12D</sup>* (Figure 6B; Supplemental Figure 4C), or in control littermates (Figure 6B; Supplemental Figure 4A). Interestingly, few PanIN lesions consisting of ducts lined with mucinous columnar epithelium that are encountered with high frequency throughout the pancreas of *Ptfla-Cre; Kras<sup>G12D</sup>* (Figure 6B; Supplemental Figure 4C) are found in *Ptfla-Cre;  $\beta$ -cat<sup>active</sup>, Kras<sup>G12D</sup>* mice.

To confirm the relative absence of PanIN lesions in *Ptfla-Cre;  $\beta$ -cat<sup>active</sup>, Kras<sup>G12D</sup>* mice, pancreas sections were

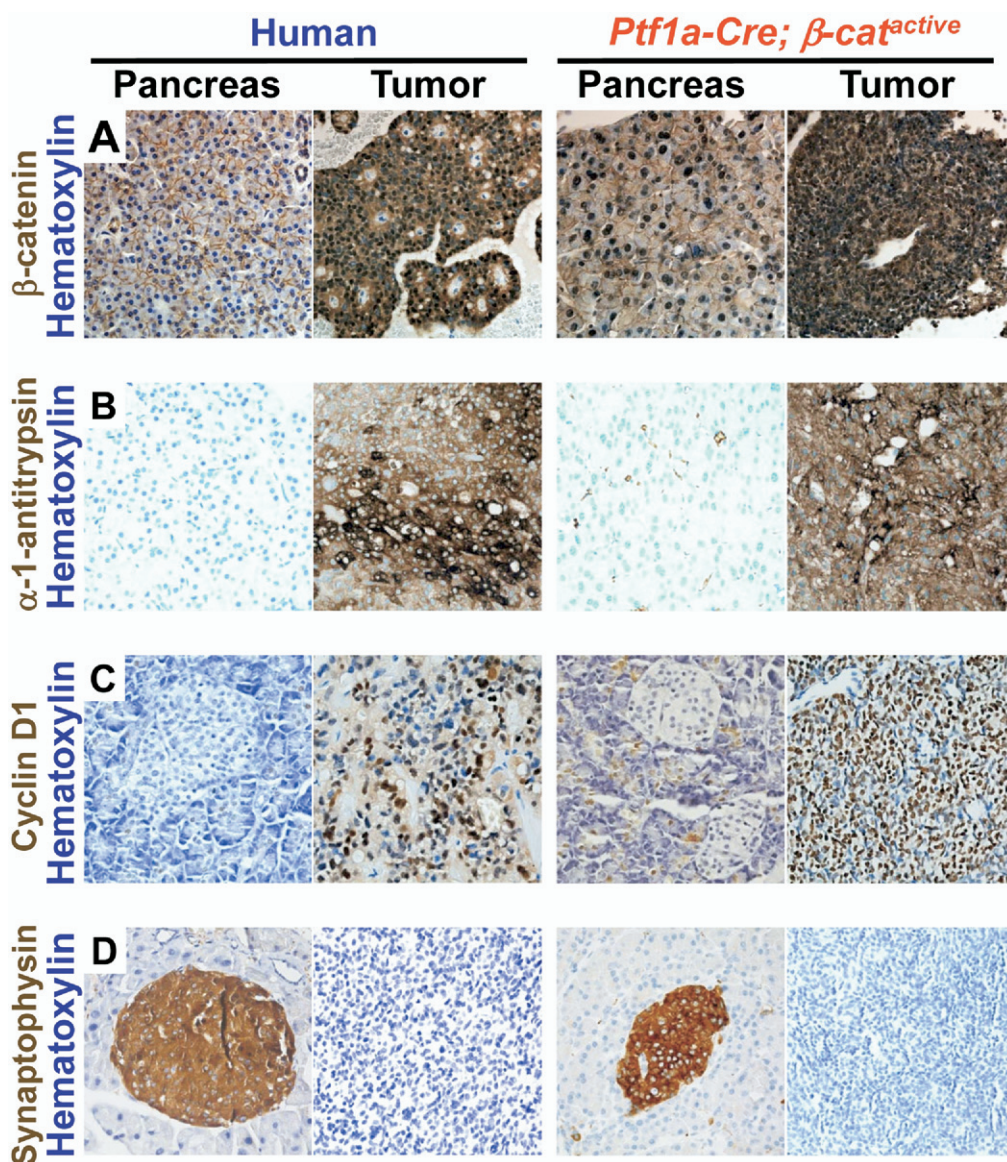


**Figure 5.** Tumors in *Ptf1a-Cre;  $\beta$ -cat<sup>active</sup>* mice have marker expression that is similar to human SPN. (A) Normal human pancreas showing membranous  $\beta$ -catenin staining and pancreas from *Ptf1a-Cre;  $\beta$ -cat<sup>active</sup>* mice exhibiting membranous and nuclear accumulation of  $\beta$ -catenin. Both human SPNs and the murine tumors show marked cytoplasmic and nuclear staining for  $\beta$ -catenin. (B)  $\alpha$ -1 Antitrypsin was expressed in human SPN and murine tumors with a globular pattern but was not expressed in normal human or *Ptf1a-Cre;  $\beta$ -cat<sup>active</sup>* pancreas. (C) Cyclin D1 was expressed at high levels in human SPN and murine tumors. Elevated levels of cyclin D1 were also detected in the exocrine tissue of the *Ptf1a-Cre;  $\beta$ -cat<sup>active</sup>* pancreas. Cyclin D1 was not detected in normal human pancreas tissue. (D) Neither human SPNs, nor murine tumors, express synaptophysin. Synaptophysin is detectable in both normal human pancreatic islets and the islets of *Ptf1a-Cre;  $\beta$ -cat<sup>active</sup>* mice. All images were acquired at high magnification (original magnification,  $\times 400$ ); tissues were counterstained with hematoxylin to improve contrast; mice were 9 months old.

stained with Alcian blue, which binds the acidic mucins produced by most PanINs. Cells with abundant Alcian blue staining are frequently detected within pancreatic ducts exhibiting PanIN morphology in the *Ptf1a-Cre; Kras<sup>G12D</sup>* mouse (Figure 6C). However, Alcian blue<sup>+</sup> cells are not present in the *Ptf1a-Cre;  $\beta$ -cat<sup>active</sup>; Kras<sup>G12D</sup>* mouse (Figure 6C, characteristic ductal lesions marked by #). Control and *Ptf1a-Cre;  $\beta$ -cat<sup>active</sup>* (Figure 6C) pancreatic tissue was also negative for Alcian blue. Similar results were obtained with periodic acid/Schiff's reagent staining, which is known to mark PanINs (data not shown), indicating that PanIN formation is blocked in *Ptf1a-Cre;  $\beta$ -cat<sup>active</sup> Kras<sup>G12D</sup>* mice.

Lesions with ductal morphology in *Ptf1a-Cre;  $\beta$ -cat<sup>active</sup>; Kras<sup>G12D</sup>* mice contained cells whose cytoplasm was intensely stained for the ductal marker cytokeratin (CK) 19 (Figure 6D, #), confirming that they have some degree of ductal differentiation. The areas of cribriform growth

pattern in *Ptf1a-Cre;  $\beta$ -cat<sup>active</sup>; Kras<sup>G12D</sup>* mice were negative for CK19 (Figure 6D, \*). Pancreatic ducts within the *Ptf1a-Cre;  $\beta$ -cat<sup>active</sup>* pancreas exhibit strong apical staining for CK19 that is equivalent to what is observed in control animals (Figure 6D). PanIN lesions in *Ptf1a-Cre; Kras<sup>G12D</sup>* mice were also strongly CK19 positive, which is consistent with previous reports<sup>34</sup> (Figure 6D).

To determine whether the tumors in the *Ptf1a-Cre;  $\beta$ -cat<sup>active</sup>; Kras<sup>G12D</sup>* mice exhibit endocrine differentiation, pancreatic sections were stained with the islet marker synaptophysin. As expected, synaptophysin staining was localized exclusively to endocrine islets in control and *Ptf1a-Cre;  $\beta$ -cat<sup>active</sup>* pancreatic tissue sections (Figure 6E). However, in addition to synaptophysin<sup>+</sup> islet structures, some scattered synaptophysin<sup>+</sup> cells were found near PanIN lesions in *Ptf1a-Cre; Kras<sup>G12D</sup>* samples (Figure 6E). Both the cribriform and ductal lesions were negative for synaptophysin in *Ptf1a-Cre;  $\beta$ -cat<sup>active</sup>; Kras<sup>G12D</sup>* samples,

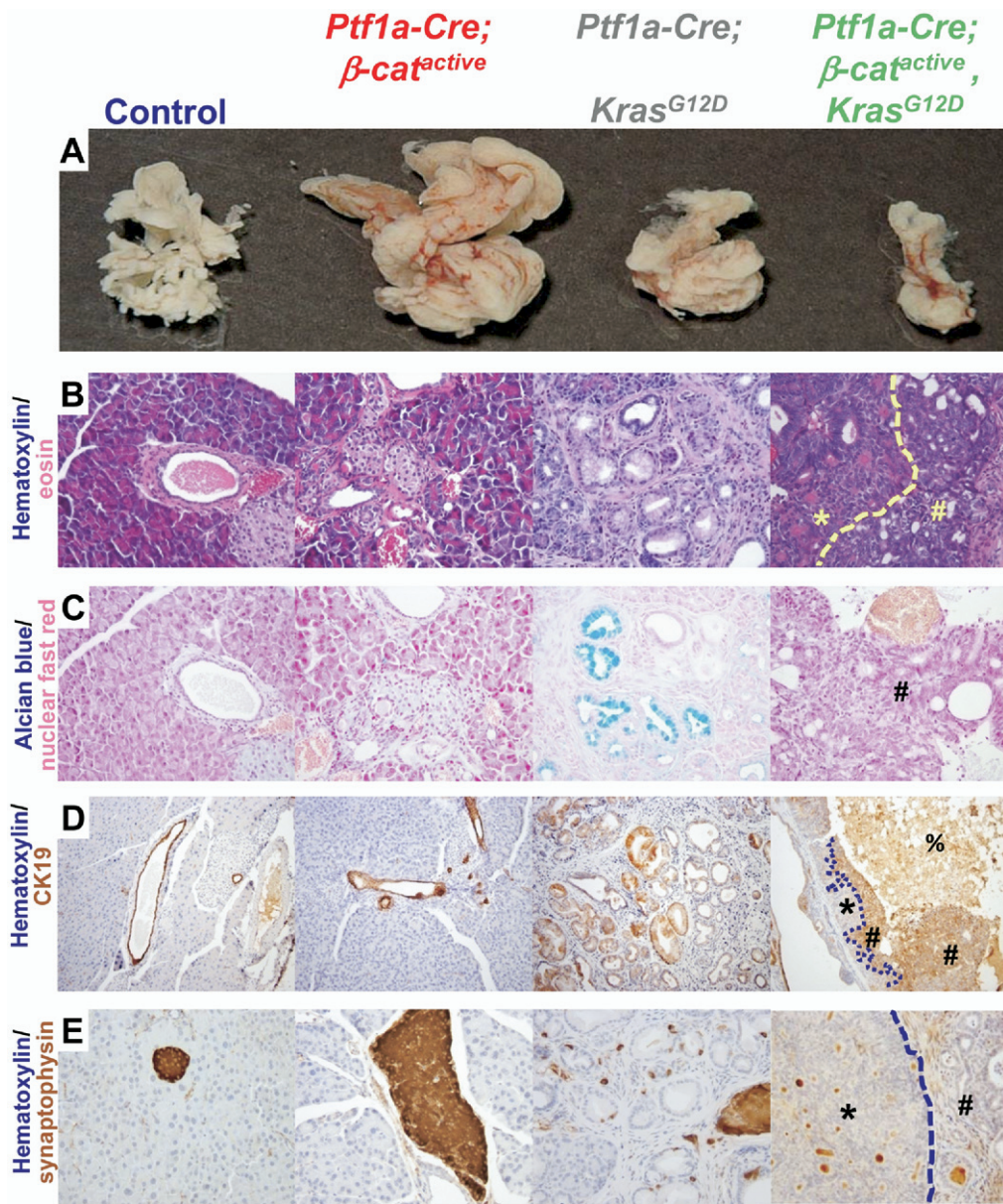


**Figure 6.** PanIN lesions do not form in *Ptf1a-Cre; β-cat<sup>active</sup>, Kras<sup>G12D</sup>* mice. (A–E) Three-month-old pancreata. (A) Pancreas size is reduced and morphology is condensed in *Ptf1a-Cre; β-cat<sup>active</sup>, Kras<sup>G12D</sup>* mice when compared with control or *Ptf1a-Cre; Kras<sup>G12D</sup>* organs. *Ptf1a-Cre; β-cat<sup>active</sup>* mice exhibit pancreatic hyperplasia in this mouse background that is equivalent to what was previously described. (B) Hematoxylin (blue) and eosin (pink) pancreas sections (original magnification, ×400). Two distinct tumor types that frequently form within *Ptf1a-Cre; β-cat<sup>active</sup>* mice have ductal (B, yellow #) or cribriform (B, yellow \*, separated by dashed yellow line) morphology. Lesions were found in all mice analyzed (*n* = 5). Similar lesions are not found in control, *Ptf1a-Cre; β-cat<sup>active</sup>*, or *Ptf1a-Cre; Kras<sup>G12D</sup>* mice. The characteristic columnar cells found within ductal lesions in the *Ptf1a-Cre; Kras<sup>G12D</sup>* are not seen in the *Ptf1a-Cre; β-cat<sup>active</sup>; Kras<sup>G12D</sup>*. (C) Alcian blue and nuclear fast red stained pancreas sections (original magnification, ×400). Alcian blue staining, a hallmark of PanIN that is apparent throughout the *Ptf1a-Cre; Kras<sup>G12D</sup>* tissue, is not seen in *Ptf1a-Cre; β-cat<sup>active</sup>, Kras<sup>G12D</sup>* mice (# ductal lesion). Alcian blue was not detected in control or *Ptf1a-Cre; β-cat<sup>active</sup>* tissue. (D) CK19 (brown) and hematoxylin (blue) stained pancreatic sections (original magnification, ×100). Normal ducts are marked by CK19 expression in control and *Ptf1a-Cre; β-cat<sup>active</sup>* pancreatic tissue, as are the characteristic PanIN lesions in the *Ptf1a-Cre; Kras<sup>G12D</sup>* pancreas. Cells with ductal morphology in the *Ptf1a-Cre; β-cat<sup>active</sup>, Kras<sup>G12D</sup>* (#) are positive for CK19. Cells with cribriform morphology do not express CK19 (\*boundary between distinct lesion types indicated by dashed line). Necrotic debris exhibits nonspecific staining (%). (E) Synaptophysin (brown) and hematoxylin (blue) stained pancreatic sections (original magnification, ×400). Pancreatic islets within control, *Ptf1a-Cre; β-cat<sup>active</sup>*, and *Ptf1a-Cre; Kras<sup>G12D</sup>* are synaptophysin positive. Neither the ductal (#) nor the cribriform (\*) lesions are synaptophysin<sup>+</sup>. Brown staining visible in the *Ptf1a-Cre; β-cat<sup>active</sup>, Kras<sup>G12D</sup>* is nonspecific staining of debris within cystic structures. Images are representative of *n* ≥ 7 samples for each mouse genotype indicated; mice were 3 months old.

suggesting a lack of endocrine differentiation (Figure 6E: \*cribriform; #ductal; brown staining within the center of some cysts is background staining caused by the presence of cellular debris).

Tumors in *Ptfla-Cre;  $\beta$ -cat<sup>active</sup>; Kras<sup>G12D</sup>* with cribriform morphology superficially resemble human acinar cell carcinoma, another rare, but aggressive, pancreatic neoplasm. Some cells within these lesions are arranged back-to-back with small lumens. The nuclei in these columnar cells are round to oval and basally located, with a moderate amount of eosinophilic cytoplasm (Figure 6B \*; higher magnifications shown in Supplemental Figure 2E and F). However, the cells are negative for markers of acinar differentiation, including amylase and chymotrypsin (data not shown). Moreover, they do not seem to have granules within the cytoplasm or the distinctively prominent nucleoli that are common hallmarks of human acinar cell carcinoma. Alternatively, these tumors display similarities to human intraductal tubular tumors (ITTs).<sup>35-37</sup> Given the rare appearance of these tumors, the presence and level of Wnt signaling has not been investigated.

Together, the histologic analysis of this cohort of mice demonstrates that activation of  $\beta$ -catenin in this particular context blocks the formation of lesions that are usually induced by Kras activation. Instead, tumor progression seems to have been shifted toward a different fate in *Ptfla-Cre;  $\beta$ -cat<sup>active</sup>; Kras<sup>G12D</sup>* mice.

### **Hh-Responsive Target Gene Expression Is Decreased in *PtflaCre $\beta$ -cat<sup>active</sup> Kras<sup>G12D</sup> Murine Lesions***

To determine how Kras activation affects  $\beta$ -catenin protein level and localization, immunohistochemistry was performed on a cohort of mouse pancreas samples at 3 months of age. The cellular concentration of  $\beta$ -catenin is significantly higher in *Ptfla-Cre;  $\beta$ -cat<sup>active</sup>; Kras<sup>G12D</sup>* tumors than it is in the *Ptfla-Cre;  $\beta$ -cat<sup>active</sup>* pancreas (Figure 7A). Moreover,  $\beta$ -catenin localization in *Ptfla-Cre;  $\beta$ -cat<sup>active</sup>; Kras<sup>G12D</sup>* is strongly cytoplasmic and nuclear, whereas it remained exclusively nuclear and membrane bound in the *Ptfla-Cre;  $\beta$ -cat<sup>active</sup>*. The further increase in  $\beta$ -catenin that occurred upon tumorigenesis in this model of Kras activation is similar to what was observed in the SPN-like tumors present in *Ptfla-Cre;  $\beta$ -cat<sup>active</sup>* mice (Figure 5A).  $\beta$ -Catenin concentration and plasma membrane localization in the *Ptfla-Cre; Kras<sup>G12D</sup>* pancreas seemed equivalent to controls (Figure 7A).

Quantitative analysis of Wnt target gene expression yielded results predicted by the level of pancreatic  $\beta$ -catenin in the different mouse samples. Up-regulation of Axin2, Tcf1, p21, and CyclinD1 expression was measured in *Ptfla-Cre;  $\beta$ -cat<sup>active</sup>* mice, with an even more robust increase occurring in *Ptfla-Cre;  $\beta$ -cat<sup>active</sup>; Kras<sup>G12D</sup>* mice (Figure 7D; Supplemental Figure 5A and B, and data not shown, respectively; see Supplementary material online at

[www.gastrojournal.org](http://www.gastrojournal.org)). Axin2 and p21 expression levels in *Ptfla-Cre; Kras<sup>G12D</sup>* mice were equivalent to control (Figure 7D; Supplemental Figure 5B, respectively), whereas Tcf1 and cyclinD1 levels were slightly elevated (Supplemental Figure 5A and data not shown, respectively). Interestingly, elevation of c-Myc was only seen in *Ptfla-Cre;  $\beta$ -cat<sup>active</sup>*, and *Ptfla-Cre;  $\beta$ -cat<sup>active</sup>; Kras<sup>G12D</sup>* remained equivalent to control (Supplemental Figure 5C).

Previous reports have shown that pancreatic activation of Kras results in up-regulation of the Hh and Notch signaling pathways.<sup>32,34,38</sup> Furthermore, this increased Hh and Notch pathway activity has been implicated in the formation of PanIN lesions and early PDA tumorigenesis.<sup>39,40</sup> Therefore, we asked whether modulation of either of these pathways in *Ptfla-Cre;  $\beta$ -cat<sup>active</sup>; Kras<sup>G12D</sup>* mice could account for the absence of PanIN formation. The majority of cells within both the cribriform and ductal lesions of the *Ptfla-Cre;  $\beta$ -cat<sup>active</sup>; Kras<sup>G12D</sup>* are positive for the Notch target gene, Hes1 (Supplemental Figure 6D and E; see Supplementary material online at [www.gastrojournal.org](http://www.gastrojournal.org)), which matches the frequency and intensity of the staining in the PanIN lesions in the *Ptfla-Cre; Kras<sup>G12D</sup>* (Supplemental Figure 6C). Hes1 staining in the *Ptfla-Cre;  $\beta$ -cat<sup>active</sup>* is equivalent to control (Supplemental Figure 6B and A respectively). This finding was confirmed by quantitative PCR (qPCR) analysis of Hes1 expression (Supplemental Figure 5D).

Immunohistochemistry for Ptc, both a Hh receptor and transcriptional target of the signaling pathway, revealed strong staining within PanIN lesions in *Ptfla-Cre; Kras<sup>G12D</sup>* (Figure 7B) mice. In contrast, no Ptc<sup>+</sup> cells were detected in *Ptfla-Cre;  $\beta$ -cat<sup>active</sup>; Kras<sup>G12D</sup>*, *Ptfla-Cre;  $\beta$ -cat<sup>active</sup>*, or control mice (Figure 7B). Similar results were obtained for the Hh ligand, Sonic Hedgehog (Shh; Figure 7C). qPCR for Ptc and Gli1, another Hh pathway target gene, as well as for Shh and Indian Hh (Ihh) supports this result. Although Ptc, Gli1, Shh, and Ihh expression is increased in *Ptfla-Cre; Kras<sup>G12D</sup>* pancreatic tissue, their expression remains equivalent to control in the *Ptfla-Cre;  $\beta$ -cat<sup>active</sup>; Kras<sup>G12D</sup>*, and *Ptfla-Cre;  $\beta$ -cat<sup>active</sup>* tissues (Supplemental Figure 5E and F; Figure 7E and F).

Previous reports have indicated that Kras activation can activate the mitogen-activated protein kinase (MAPK) and PI3 kinase pathways.<sup>38</sup> Therefore, we asked whether simultaneous activation of  $\beta$ -catenin and Kras in the *Ptfla-Cre;  $\beta$ -cat<sup>active</sup>; Kras<sup>G12D</sup>* pancreas affected either MAPK or PI3 kinase activity. Western blotting of pancreatic lysates indicated that the level of MAPK phosphorylation in *Ptfla-Cre;  $\beta$ -cat<sup>active</sup>; Kras<sup>G12D</sup>* was equivalent to that seen in *Ptfla-Cre; Kras<sup>G12D</sup>*; phosphorylated MAPK could not be detected in either control or *Ptfla-Cre;  $\beta$ -cat<sup>active</sup>* pancreatic tissue (Supplemental Figure 7; see Supplementary material online at [www.gastrojournal.org](http://www.gastrojournal.org)). However, an increase in Akt phosphorylation, a read-out of PI3 kinase activity, that is seen in *Ptfla-Cre;*

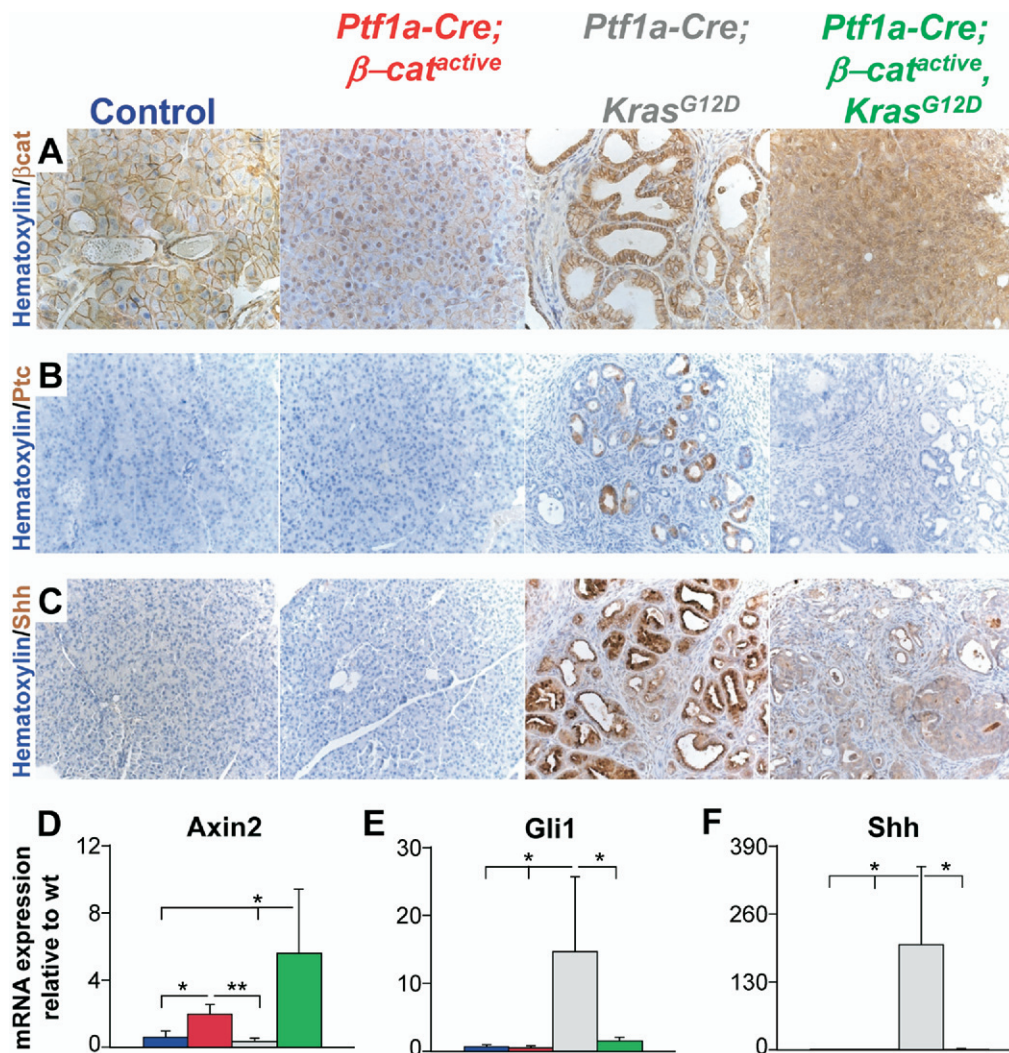


**Figure 7.** Hh-responsive target gene expression is decreased in *Ptf1aCre  $\beta$ -cat<sup>active</sup> Kras<sup>G12D</sup>* murine lesions. (A)  $\beta$ -Catenin (brown) and hematoxylin (blue) stained pancreatic sections.  $\beta$ -Catenin is preferentially localized to the plasma membrane and nucleus within the pancreas of *Ptf1a-Cre;  $\beta$ -cat<sup>active</sup>*. Lesions within the *Ptf1a-Cre;  $\beta$ -cat<sup>active</sup>, Kras<sup>G12D</sup>* mice exhibit even stronger nuclear staining for  $\beta$ -catenin, along with high levels of cytoplasmic staining.  $\beta$ -Catenin remains localized only to the plasma membrane in control and *Ptf1a-Cre; Kras<sup>G12D</sup>* pancreata. (B) Ptc (brown) and hematoxylin (blue) stained pancreatic sections. Cells within PanIN lesions in the *Ptf1a-Cre; Kras<sup>G12D</sup>* show strong Ptc staining. Ptc staining in the *Ptf1a-Cre;  $\beta$ -cat<sup>active</sup>, Kras<sup>G12D</sup>* lesion is equivalent to the background staining seen in control and *Ptf1a-Cre;  $\beta$ -cat<sup>active</sup>* pancreata. (C) Shh (brown) and hematoxylin (blue) stained pancreatic sections. Robust staining for Shh ligand is seen in the majority of the remaining epithelial cells and PanIN lesions in the *Ptf1a-Cre; Kras<sup>G12D</sup>* pancreas. Shh staining within the lesions in the *Ptf1a-Cre;  $\beta$ -cat<sup>active</sup>, Kras<sup>G12D</sup>* is only slightly higher than the background staining in control and *Ptf1a-Cre;  $\beta$ -cat<sup>active</sup>* pancreata. (D–F) Graphs showing quantitative PCR normalized to wild-type control; control (blue); *Ptf1a-Cre;  $\beta$ -cat<sup>active</sup>* (red); *Ptf1a-Cre; Kras<sup>G12D</sup>* (grey); and *Ptf1a-Cre;  $\beta$ -cat<sup>active</sup>, Kras<sup>G12D</sup>* (green). Significant up-regulation of the canonical Wnt target gene *Axin2* was detected in *Ptf1a-Cre;  $\beta$ -cat<sup>active</sup>* murine pancreatic tissue when compared with control and *Ptf1a-Cre; Kras<sup>G12D</sup>* pancreas (D). Further up-regulation of these target genes was measured in *Ptf1a-Cre;  $\beta$ -cat<sup>active</sup>, Kras<sup>G12D</sup>* pancreatic tissue when compared with the *Ptf1a-Cre;  $\beta$ -cat<sup>active</sup>* (D). Significant up-regulation of the Hh-responsive target genes *Gli1* was seen only in the *Ptf1a-Cre; Kras<sup>G12D</sup>* (E). mRNA expression of *Gli1* was equivalent in control, *Ptf1a-Cre;  $\beta$ -cat<sup>active</sup>*, and *Ptf1a-Cre;  $\beta$ -cat<sup>active</sup>, Kras<sup>G12D</sup>* pancreatic tissue (E). Strong up-regulation of the Hh ligand, *Shh*, was also detected exclusively in *Ptf1a-Cre; Kras<sup>G12D</sup>* samples (F). No significant increase in the expression of this ligand was found in control, *Ptf1a-Cre;  $\beta$ -cat<sup>active</sup>*, or *Ptf1a-Cre;  $\beta$ -cat<sup>active</sup>, Kras<sup>G12D</sup>* samples (F). All image data shown in this figure came from 3-month-old mice. Images are representative of  $n \geq 7$  samples for each mouse genotype indicated. Quantitative PCR was conducted on mRNA isolated from  $n = 3$  animals from each genotype. Error bars represent standard deviation. Confidence intervals were calculated using Student's *t*-test. *P* values: #not significant; \**P* < .05; \*\**P* < .01; mice were 3 months old.

*Kras<sup>G12D</sup>* (2 out of 3 animals) does not occur in *Ptf1a-Cre;  $\beta$ -cat<sup>active</sup>, Kras<sup>G12D</sup>* littermates (0 of 3 animals; Supplemental Figure 7). Instead, pAKT levels in the *Ptf1a-Cre;  $\beta$ -cat<sup>active</sup>, Kras<sup>G12D</sup>* and *Ptf1a-Cre;  $\beta$ -cat<sup>active</sup>* animals seem equivalent to controls (Supplemental Figure 7). Therefore, increased

canonical Wnt signaling may block *Kras*-dependent activation of PI3 kinase.

Thus, stabilization of  $\beta$ -catenin in the presence of an activating mutation in *Kras* results in a dramatic increase in canonical Wnt signaling and Notch signaling. Conse-

quently, Kras activation no longer induces up-regulation of the Hh signaling pathway and Akt phosphorylation. Further experimentation is necessary to elucidate a mechanism to explain the molecular changes we have observed. However, it seems possible that these changes may partially explain the absence of PanIN lesions in *Ptf1a-Cre*;  $\beta$ -cat<sup>active</sup>, *Kras*<sup>G12D</sup> mice.

## Discussion

Solid-pseudopapillary neoplasms are a rare human neoplasm that account for approximately 1% of pancreatic tumors.<sup>41</sup> Various groups have reported that >90% of these tumors contain mutations that are predicted to interfere with the serine/threonine phosphorylation that is necessary to properly target  $\beta$ -catenin for degradation.<sup>18,42</sup> Similar loss of this phosphorylation in  $\beta$ -cat<sup>active</sup> mice, through Cre-mediated loss of the third exon, results in large tumors that seem to be closely related to human SPN. Thus, this study demonstrates for the first time that these human mutations in  $\beta$ -catenin are likely the proximate cause of SPN. Moreover, the *Ptf1a-Cre*;  $\beta$ -cat<sup>active</sup> mouse is the first published murine model of this enigmatic tumor and proves that  $\beta$ -catenin stabilization, alone, is sufficient to induce SPN tumorigenesis within the appropriate cellular context. Interestingly, human SPNs most often occur in young females.<sup>41</sup> However, tumor frequency was equivalent in male and female mice and advanced with age in the *Ptf1a-Cre*;  $\beta$ -cat<sup>active</sup> mouse. This suggests that there might be different modifiers that alter human susceptibility to this pancreatic tumor.

Lineage tracing experiments are necessary to conclusively demonstrate that pancreatic ducts are the cells of origin in the SPN-like tumors we describe in the *Ptf1a-Cre*;  $\beta$ -cat<sup>active</sup> mice. Unfortunately, efforts to create a mouse strain in which Cre-recombinase activity is restricted to the pancreatic ductal compartment have been unsuccessful so far. However, comparing the phenotype we observe in the *Ptf1a-Cre*;  $\beta$ -cat<sup>active</sup> with that of the *Pdx-Cre<sup>late</sup>*;  $\beta$ -cat<sup>active28</sup> provides compelling, although not definitive, evidence of a ductal origin for SPN. *Pdx-Cre<sup>late</sup>* mice have Cre-recombinase activity in acinar cells and pancreatic islets, but not within pancreatic ducts. The pancreas of *Pdx-Cre<sup>late</sup>*;  $\beta$ -cat<sup>active</sup> mice grows to nearly 5 times the size of control littermates owing to expansion of the exocrine compartment, a phenotype similar to that seen in *Ptf1a-Cre*;  $\beta$ -cat<sup>active</sup> mice. In contrast, tumors did not develop in *Pdx-Cre<sup>late</sup>*;  $\beta$ -cat<sup>active</sup> mice or in another model of pancreatomegaly that is based on the conditional elimination of APC.<sup>43</sup> Conversely, *Ptf1a-Cre*;  $\beta$ -cat<sup>active</sup> mice successfully activate  $\beta$ -catenin within pancreatic ducts, in addition to the islet and acinar compartments, resulting in a high frequency of SPN-like tumors. Although one cannot rule out the existence of a previously unappreciated cell population that is being selectively targeted by the *Ptf1a-Cre* and not the *PdxCre<sup>late</sup>* mouse

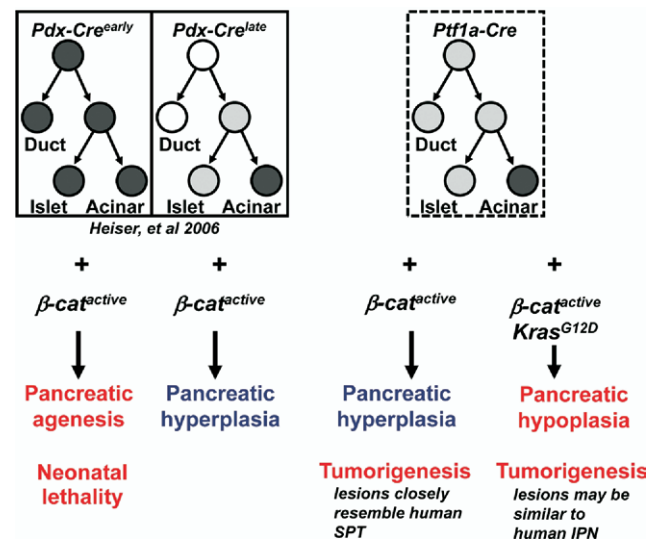


**Figure 8.** Comparison of Cre expression domains of *Pdx-Cre<sup>early</sup>*, *Pdx-Cre<sup>late</sup>*, and *Ptf1a-Cre*. Schematic illustrates the cellular compartments targeted by the different pancreatic mouse Cre strains, and their respective phenotype when crossed to the  $\beta$ -cat<sup>active</sup> mouse. White circles indicate no Cre expression. Light gray circles indicate mosaic Cre expression. Dark gray circles indicate robust Cre expression.

strain, it is likely that cells residing within the ductal compartment are responsible for the tumors observed. A schematic of the expression domains of the various mouse Cre strains we have used to stabilize  $\beta$ -catenin and their resultant phenotype is provided in Figure 8.

Our finding that concurrent activation of  $\beta$ -catenin in the *Kras*<sup>G12D</sup> mouse diverts the cellular fate of neoplasms from PanINs to novel ductal and cribriform tumor isoforms was particularly surprising. The *Ptf1a-Cre*; *Kras*<sup>G12D</sup> mouse model has proven to be especially permissive to the formation of PDA in mice. The introduction of a variety of oncogenic mutations, such as the loss of the tumor suppressors p53 or Ink4a/Arf,<sup>34,44</sup> into this model results in the formation of tumors with differing degrees of malignancy. More recently it has been shown that the introduction of other mutations in the *Ptf1a Cre*; *Kras*<sup>G12D</sup> mouse model can shift the formation of PanIN lesions toward the formation of cystic neoplasms. The combination of a Kras mutation and Dpc4/Smad4 mutations in the mice results in the formation of mucinous cystic neoplasms and intraductal papillary mucinous neoplasms, respectively.<sup>45,46</sup> These recently recognized entities are also thought to give rise to PDAC. In contrast with the Kras/DPC4-induced aberrations, the lesions we observed in *Ptf1aCre*;  $\beta$ -cat<sup>active</sup>; *Kras*<sup>G12D</sup> are not mucinous. Therefore, the activation of  $\beta$ -catenin in the context of a Kras-activating mutation prevents the formation of PanIN lesions while resulting in other neoplastic alterations. The exact nature of these tumors remains to be established, but their ductal properties display similarities to recently defined ITTs,<sup>35-37</sup> a subgroup of intraductal neoplasms possibly related to intraductal papillary-

mucinous neoplasms. However, because these ITTs have only recently been described, a direct comparison between *Ptf1a-Cre*;  $\beta$ -cat<sup>active</sup>; *Kras*<sup>G12D</sup> mouse and human tumors will need to be addressed in future studies. A discriminating feature of the tumors observed in the *Ptf1a-Cre*;  $\beta$ -cat<sup>active</sup>; *Kras*<sup>G12D</sup> mice is the absence of Hh signaling that is seen in PanIN lesions. It will be interesting to investigate the status of Hh signaling in human ITTs.

In conclusion, our study demonstrates that the context and sequence in which oncogenic mutations are acquired in the pancreas have a profound impact on tumor initiation and outcome. Moreover, our results suggest that the Wnt signaling pathway may act as a key determinant of tumor fate within the pancreas. Human PDA is the fourth leading cause of cancer death in the United States. Current therapies are ineffective in treating this malignancy, resulting in a 5-year survival rate that is <5%. Our observation that stabilization of  $\beta$ -catenin dramatically alters the tumor phenotype in a mouse model of early PDA provides another window into the complex molecular circuitry involved in tumorigenesis. Further dissection of how  $\beta$ -catenin activation alters the downstream consequences of *Kras* activation might lead to novel therapeutic opportunities.

### Supplementary Data

Note: To access the supplementary material accompanying this article, visit the online version of *Gastroenterology* at [www.gastrojournal.org](http://www.gastrojournal.org), and at doi: [10.1053/j.gastro.2008.06.089](https://doi.org/10.1053/j.gastro.2008.06.089).

### References

- Gregorieff A, Clevers H. Wnt signaling in the intestinal epithelium: from endoderm to cancer. *Genes Dev* 2005;19:877–890.
- Fodde R, Brabletz T. Wnt/beta-catenin signaling in cancer stemness and malignant behavior. *Curr Opin Cell Biol* 2007;19:150–158.
- Polakis P. The many ways of Wnt in cancer. *Curr Opin Gene Dev* 2007;17:45–51.
- Reya T, Clevers H. Wnt signalling in stem cells and cancer. *Nature* 2005;434:843–850.
- Widelitz R. Wnt signaling through canonical and non-canonical pathways: recent progress. *Growth Factors* 2005;23:111–116.
- Murtaugh LC, Law AC, Dor Y, et al. Beta-catenin is essential for pancreatic acinar but not islet development. *Development* 2005;132:4663–4674.
- Papadopoulou S, Edlund H. Attenuated Wnt signaling perturbs pancreatic growth but not pancreatic function. *Diabetes* 2005;54:2844–2851.
- Dessimoz J, Bonnard C, Huelsken J, et al. Pancreas-specific deletion of beta-catenin reveals Wnt-dependent and Wnt-independent functions during development. *Curr Biol* 2005;15:1677–1683.
- Wells JM, Esni F, Boivin GP, et al. Wnt/beta-catenin signaling is required for development of the exocrine pancreas. *BMC Dev Biol* 2007;7:4.
- Heller RS, Dichmann DS, Jensen J, et al. Expression patterns of Wnts, Frizzleds, sFRPs, and misexpression in transgenic mice suggesting a role for Wnts in pancreas and foregut pattern formation. *Dev Dyn* 2002;225:260–270.
- Koesters R, von Knebel Doeberitz M. The Wnt signaling pathway in solid childhood tumors. *Cancer Lett* 2003;198:123–138.
- Abraham SC, Wu TT, Hruban RH, et al. Genetic and immunohistochemical analysis of pancreatic acinar cell carcinoma: frequent allelic loss on chromosome 11p and alterations in the APC/beta-catenin pathway. *Am J Pathol* 2002;160:953–962.
- Al-Aynati MM, Radulovich N, Riddell RH, et al. Epithelial-cadherin and beta-catenin expression changes in pancreatic intraepithelial neoplasia. *Clin Cancer Res* 2004;10:1235–1240.
- Lowy AM, Fenoglio-Preiser C, Kim OJ, et al. Dysregulation of beta-catenin expression correlates with tumor differentiation in pancreatic duct adenocarcinoma. *Ann Surg Oncol* 2003;10:284–290.
- Zeng G, Germinaro M, Micsenyi A, et al. Aberrant Wnt/beta-catenin signaling in pancreatic adenocarcinoma. *Neoplasia* 2006;8:279–289.
- Nishimori I, Kohsaki T, Tochika N, et al. Non-cystic solid-pseudopapillary tumor of the pancreas showing nuclear accumulation and activating gene mutation of beta-catenin. *Pathol Int* 2006;56:707–711.
- Min Kim S, Sun CD, Park KC, et al. Accumulation of beta-catenin protein, mutations in exon-3 of the beta-catenin gene and a loss of heterozygosity of 5q22 in solid pseudopapillary tumor of the pancreas. *J Surg Oncol* 2006;94:418–425.
- Abraham SC, Klimstra DS, Wilentz RE, et al. Solid-pseudopapillary tumors of the pancreas are genetically distinct from pancreatic ductal adenocarcinomas and almost always harbor beta-catenin mutations. *Am J Pathol* 2002;160:1361–1369.
- Cao D, Maitra A, Saavedra JA, et al. Expression of novel markers of pancreatic ductal adenocarcinoma in pancreatic nonductal neoplasms: additional evidence of different genetic pathways. *Mod Pathol* 2005;18:752–761.
- Harada N, Tamai Y, Ishikawa T, et al. Intestinal polyposis in mice with a dominant stable mutation of the beta-catenin gene. *EMBO J* 1999;18:5931–5942.
- Hingorani SR, Petricoin EF, Maitra A, et al. Preinvasive and invasive ductal pancreatic cancer and its early detection in the mouse. *Cancer Cell* 2003;4:437–450.
- Soriano P. Generalized lacZ expression with the ROSA26 Cre reporter strain. *Nat Genet* 1999;21:70–71.
- Lobe CG, Koop KE, Kreppner W, et al. Z/AP, a double reporter for cre-mediated recombination. *Dev Biol* 1999;208:281–292.
- Kawaguchi Y, Cooper B, Gannon M, et al. The role of the transcriptional regulator Ptf1a in converting intestinal to pancreatic progenitors. *Nat Genet* 2002;32:128–134.
- Gu G, Dubauskaite J, Melton DA. Direct evidence for the pancreatic lineage: NGN3+ cells are islet progenitors and are distinct from duct progenitors. *Development* 2002;129:2447–2457.
- Kawahira H, Ma NH, Tzanakakis ES, et al. Combined activities of hedgehog signaling inhibitors regulate pancreas development. *Development* 2003;130:4871–4879.
- Kim SK, Hebrok M, Melton DA. Notochord to endoderm signaling is required for pancreas development. *Development* 1997b;124:4243–4252.
- Heiser PW, Lau J, Taketo MM, et al. Stabilization of beta-catenin impacts pancreas growth. *Development* 2006;133:2023–2032.
- Jaffee EM, Hruban RH, Canto M, et al. Focus on pancreas cancer. *Cancer Cell* 2002;2:25–28.
- Tuveson DA, Hingorani SR. Ductal pancreatic cancer in humans and mice. *Cold Spring Harb Symp Quant Biol* 2005;70:65–72.
- Hezel AF, Kimmelman AC, Stanger BZ, et al. Genetics and biology of pancreatic ductal adenocarcinoma. *Genes Dev* 2006;20:1218–1249.

32. Zhu L, Shi G, Schmidt CM, et al. Acinar cells contribute to the molecular heterogeneity of pancreatic intraepithelial neoplasia. *Am J Pathol* 2007;171:263–273.
33. Aguirre AJ, Bardeesy N, Sinha M, et al. Activated Kras and Ink4a/Arf deficiency cooperate to produce metastatic pancreatic ductal adenocarcinoma. *Genes Dev* 2003;17:3112–3126.
34. Hingorani SR, Wang L, Multani AS, Combs C, et al. Trp53R172H and KrasG12D cooperate to promote chromosomal instability and widely metastatic pancreatic ductal adenocarcinoma in mice. *Cancer Cell* 2005;7:469–483.
35. Tajiri T, Tate G, Inagaki T, Kunimura T, et al. Intraductal tubular neoplasms of the pancreas: histogenesis and differentiation. *Pancreas* 2005;30:115–121.
36. Albores-Saavedra J, Sheahan K, O'Riain C, et al. Intraductal tubular adenoma, pyloric type, of the pancreas: additional observations on a new type of pancreatic neoplasm. *Am J Surg Pathol* 2004;28:233–238.
37. Tajiri T, Tate G, Kunimura T, et al. Histologic and immunohistochemical comparison of intraductal tubular carcinoma, intraductal papillary-mucinous carcinoma, and ductal adenocarcinoma of the pancreas. *Pancreas* 2004;29:116–122.
38. Pasca di Magliano M, Sekine S, Ermilov A, et al. Hedgehog/Ras interactions regulate early stages of pancreatic cancer. *Genes Dev* 2006;20:3161–3173.
39. Thayer SP, di Magliano MP, Heiser PW, et al. Hedgehog is an early and late mediator of pancreatic cancer tumorigenesis. *Nature* 2003;425:851–856.
40. Miyamoto Y, Maitra A, Ghosh B, et al. Notch mediates TGF alpha-induced changes in epithelial differentiation during pancreatic tumorigenesis. *Cancer Cell* 2003;3:565–576.
41. Klimstra DS, Wenig BM, Heffess CS. Solid-pseudopapillary tumor of the pancreas: a typically cystic carcinoma of low malignant potential. *Semin Diagn Pathol* 2000;17:66–80.
42. Tanaka Y, Kato K, Notohara K, et al. Frequent beta-catenin mutation and cytoplasmic/nuclear accumulation in pancreatic solid-pseudopapillary neoplasm. *Cancer Res* 2001;61:8401–8404.
43. Strom A, Bonal C, Ashery-Padan R, et al. Unique mechanisms of growth regulation and tumor suppression upon Apc inactivation in the pancreas. *Development* 2007;134:2719–2725.
44. Bardeesy N, Aguirre AJ, Chu GC, et al. Both p16(Ink4a) and the p19(Arf)-p53 pathway constrain progression of pancreatic adenocarcinoma in the mouse. *Proc Natl Acad Sci U S A* 2006;103:5947–5952.
45. Bardeesy N, Cheng KH, Berger JH, et al. Smad4 is dispensable for normal pancreas development yet critical in progression and tumor biology of pancreas cancer. *Genes Dev* 2006;20:3130–3146.
46. Izeradjene K, Combs C, Best M, et al. Kras(G12D) and Smad4/Dpc4 haploinsufficiency cooperate to induce mucinous cystic neoplasms and invasive adenocarcinoma of the pancreas. *Cancer Cell* 2007;11:229–243.

---

Received December 14, 2007. Accepted June 19, 2008.

Address requests for reprints to: Matthias Hebrok, 513 Parnassus Ave, HSW 1116, Box 0540 San Francisco, CA 94143. e-mail: [mhebrok@diabetes.ucsf.edu](mailto:mhebrok@diabetes.ucsf.edu); fax: 415-564-5813.

Supported by the NIH (CA112537) and the American Diabetes Association.

The authors are indebted to Drs Doug Melton, Chris Wright, Sunil Hingorani, and David Tuveson for providing the *Pdx-Cre<sup>early</sup>*, *Ptf1a-Cre* mouse strains, and *Kras<sup>G12D</sup>*, respectively, and to Dr Mike German for providing the Pdx1 antibody. We also thank Drs Mike German and Gail Martin for helpful discussions, Jane Milliken for help with the human SPN immunohistochemistry, Micah Allen for histology support, Heather Heiser for the maintenance of our mouse stocks, and Don and Marcia Trask for imaging assistance. Work in M.H.'s laboratory was supported by grants from the NIH (CA112537, DK60533) and the American Diabetes Association. P.W.H. was a part of the UCSF Biomedical Science graduate student program when this research was conducted. D.A.C. was supported by a postdoctoral fellowship from the California Institute of Regenerative Medicine (CiRM). L.L. was supported by a postdoctoral fellowship from the Juvenile Diabetes Research Foundation. Confocal and other images were generated in the UCSF Diabetes and Endocrinology Research Center microscopy core (P30 DK63720).